Double-Bond-induced Morphotropic Phase Boundary leads to Enhanced Electrocaloric Effect in VDF-Based Polymer Flexible Devices

Florian Le Goupil, Konstantinos Kallitsis, Sylvie Tencé-Girault, Cyril Brochon, Eric Cloutet, Guillaume Fleury, Georges Hadziioannou

Double-Bond-induced Morphotropic Phase Boundary leads to Enhanced Electrocaloric Effect in VDF-based Polymer Flexible Devices.

Florian Le Goupil[a*], Konstantinos Kallitsis[a,b], Sylvie Tencé-Girault[c,d], Cyril Brochon[a], Eric Cloutet[a], Guillaume Fleury[a], and Georges Hadziioannou[a*]

[a] *LCPO, University of Bordeaux, CNRS, Bordeaux INP, UMR 5629, F-33600, Pessac, France*

[b]*Department of Chemical Engineering and Biotechnology, University of Cambridge, Cambridge, CB3 0AS, United Kingdom.*

[c]*Laboratoire PIMM, Arts et Metiers Institute of Technology, CNRS, Cnam, HESAM University, 151 Bd de l'Hopital, 75013 Paris, France*

[d]*Arkema, CERDATO, Route du Rilsan, 27470 Serquigny, France*

*Email: florian.le-goupil@u-bordeaux.fr

*Email: georges.hadziioannou@u-bordeaux.fr

Abstract: Electrocaloric (EC) polymers answer the needs for green, efficient, and flexible coolers, as well as thermal management in wearable electronics. A morphotropic phase boundary is induced for the first time in P(VDF-*ter*-TrFE-*ter*-CFE) polymers near room temperature, by soft one-pot addition of small fractions of double bonds. It results in flexible devices with remarkable cooling performance, ΔT_{EC} = 5.8 K for E < 100 MV·m^{-1} and up to 9.3 K at higher fields, which are maintained when bent to various angles required for wearable electronics. This work paves the way for the development of scalable, high-performance, flexible organic cooling devices.

Keywords: electrocaloric effect, relaxor ferroelectrics, phase transitions, polymers, flexible devices, wearable electronics.

Introduction

The refrigeration and cooling industry (RC) is one of the main sources of greenhouse gases emissions, and the situation is expected to worsen with rising global temperatures. Low-efficiency and high-global warming impact technologies must be phased-out from the RC. With theoretical efficiency over 80%,[1,2] solid-state cooling based on the electrocaloric (EC) effect has emerged as a serious candidate to facilitate this transition, but its potential for applications is still hindered by the low performance of EC materials. EC cooling is based on the electrocaloric effect (ECE), which arises from the increase of the net polarization in polar crystals, upon the application of an external electric field, *E*. Under adiabatic conditions, the system compensates the decrease of dipolar entropy (inherent to the alignment of dipoles) with an increase in lattice vibration entropy, *i.e.* an adiabatic temperature increase, ΔT_{EC}, thus keeping the overall entropy of the system constant.[1] In a hysteresis-free environment (remanent polarisation, $P_r \sim 0$), this process is fully reversible, and an equivalent

cooling power is obtained upon removing the electric field. ΔT_{EC}, which governs the cooling power produced by the electrocaloric material, depends on several material specific dielectric properties, the main one being the polarization, P.[1,3,4] A high maximum polarization P_{max} is thus required to induced a large ΔT_{EC}, while a high relative permittivity, ε_r ,which dictates dP/dE, ensures the efficiency of the process, by keeping the applied field sufficiently low.

Inorganic materials, especially oxide perovskites with highly composition-dependent phase transitions temperatures such as (1-x)Pb($Mg_{1/3}Nb_{2/3}$)O_3-x$PbTiO_3$ (PMN-PT) and $BaZr_xTi_{1-x}O_3$ (BZT) solid solutions display remarkable electromechanical responses in specific regions of their phase diagrams,[5–9] where enhanced ECE have been reported.[10–14] In these compositional regions, referred to as morphotropic phase boundaries (MPB) or phase convergence regions, several polar/non-polar phases coexist due to a decrease of the energy barrier separating them.[5–7,15] This leads to a crossover region between ferroelectric (FE) and relaxor ferroelectric (RFE) behaviours where huge changes in dipolar entropy can be induced by applying only moderate electric fields, hence the enhanced ECE.

Only a few studies have reported MPBs in organic polymers such as poly(vinylidenefluoride-*co*-trifluoroethylene) P(VDF-*co*-TrFE) copolymers.[16,17] Improved dielectric properties were observed in the crossover region from the FE behaviour to the RFE behaviour, (i.e. near the 50/50 composition), as a result of a drastic decrease in the activation energy to flip between equivalent dipolar directions.[16,17]

These highly polar polymers are promising for various application as they are non-volatile, their production is low-cost and scalable, but also due to their flexibility. Their viscoelastic mechanical properties allow them to be used solid-state cooling as both the cooling source and the driving force to extract the heat, by exploiting electrostatic actuation.[18] Their flexibility also has implications for printed electronics, which is widely regarded as the route toward cheap, large-area, flexible and easily scalable electronics.[19] Carbon-based circuit boards including transistors,

capacitors and resistors can now be printed with competitive performance, which is especially interesting for the development of wearable electronics. However, the extra temperature sensitivity resulting from their organic nature has made thermal management in these components all the more critical, thus making flexible and printable electrocaloric coolers highly desirable.

Unfortunately, the aforementioned P(VDF-*co*-TrFE) (50/50) displays large polarisation hysteresis and its phase transition from the polar to non-polar phase, where the dielectric permittivity is maximised, sits near 70 °C. This limits its potential for applications in cooling wearable electronics, where devices must be efficient from room temperature (RT, 25 °C) to body temperature (36 °C to 40 °C).[19]

The addition of a third co-monomer to P(VDF-*co*-TrFE), such as chlorofluoro-ethylene (CFE), also induces the crossover from FE to RFE, while significantly lowering the phase transition temperature. Consequently, a complete crossover to the RFE behaviour is obtained in Poly(vinylidenefluoride-*ter*-trifluoroethylene-*ter*-chlorofluoro-ethylene) P(VDF-*ter*-TrFE-*ter*-CFE) (63/30/7) with a phase transition near RT. It displays a remarkably high permittivity, $\varepsilon_r \sim 50$, with low hysteresis ($P_r \sim 0$), making it the most promising polymer for ECE cooling with reported $\Delta T_{EC} \sim 3$ K at a moderate field of 60 MV·m^{-1}.[18,20,21] Several strategies have been explored to further increase the ECE of these state-of-the-art materials. Among them, blending with VDF-rich P(VDF-*co*-TrFE) has yielded good results with $\Delta T_{EC} = 4$ K reported at 60 MV·m^{-1}.[20] We have also shown that the ECE could be enhanced in terpolymers with chlorotrifluoroethylene (CTFE) by finely engineering their structure through the introduction of unsaturation on the polymer backbone, leading to over 60% enhancement in ΔT_{EC} near room temperature.[4] Our approach has recently been shown to also be successful in CFE-based terpolymers.[22]

Here we show that the dielectric and electrocaloric properties in P(VDF-*ter*-TrFE-*ter*-CFE) (63/30/7) can be further enhanced by slightly reverting the RFE to FE crossover, which induces a morphotropic phase boundary near room temperature. This is achieved by introducing minute

amounts of double bounds to induce a highly polar polymer chain configuration, in the vicinity of which dipole rotation is facilitated upon electric field application. We also show that the enhanced dielectric properties of these flexible material are maintained when bent to angles typically used for wearable electronics.

Results and discussion

The dielectric properties of P(VDF-*ter*-TrFE-*ter*-CFE) were finely tuned through the introduction of minute amount of unsaturation (C=C double bonds) on the polymer backbone (Fig. 1a). The dehydrochlorination of the terpolymers, which is schematically represented in Scheme S1, was induced by reacting with a weak base (triethyl amine), similarly to the approach use in our previous work.[4] The double bond (DB) content was identified with ^{1}H NMR (Fig. S1) and found to vary between 0.1% and 2.5%, depending on the conditions used during the chemical modification (Table S1). The DB introduction further enhanced the dielectric permittivity of the modified P(VDF-*ter*-TrFE-*ter*-CFE), with the maximum permittivity ε_{max} increasing from 51 for the pristine terpolymer to 52, 55 and 54, for 0.1% DB, 0.2% DB and 0.9% DB-modified polymers, respectively (1 kHz, Fig. 1b). The temperature of the maximum permittivity also increased slightly, from 29 °C for the pristine terpolymers to 31 °C and 33 °C for 0.2% DB and 0.9% DB-modified polymers, respectively. Although it also induced a high permittivity, increasing the DB content to 2.5%, significantly affected the shape of the dielectric response with temperature, with a clear crossover to a sharper ferroelectric-type transition. This led to a significant drop in ε_r at 25 °C and a drastic shift of the maximum to higher temperature. The DB-induced enhancement of the dielectric properties was maintained at high field with a slight increase of the maximum polarisation measured at 120 MV·m^{-1} in the terpolymers modified with small amount of DBs (Fig. 1c). While the highest polarisation is measured in the 0.9% DB modified polymer, this composition also displays an

increased hysteresis (higher remanent polarisation, P_r) with more energy lost (area inside the *P-E* loop) during the capacitor discharge, U_{loss}= 0.6 J·cm^{-3}, than for the pristine polymer or the ones with lower DB contents, U_{loss} = 0.4 J·cm^{-3} (inset of Fig. 1c).

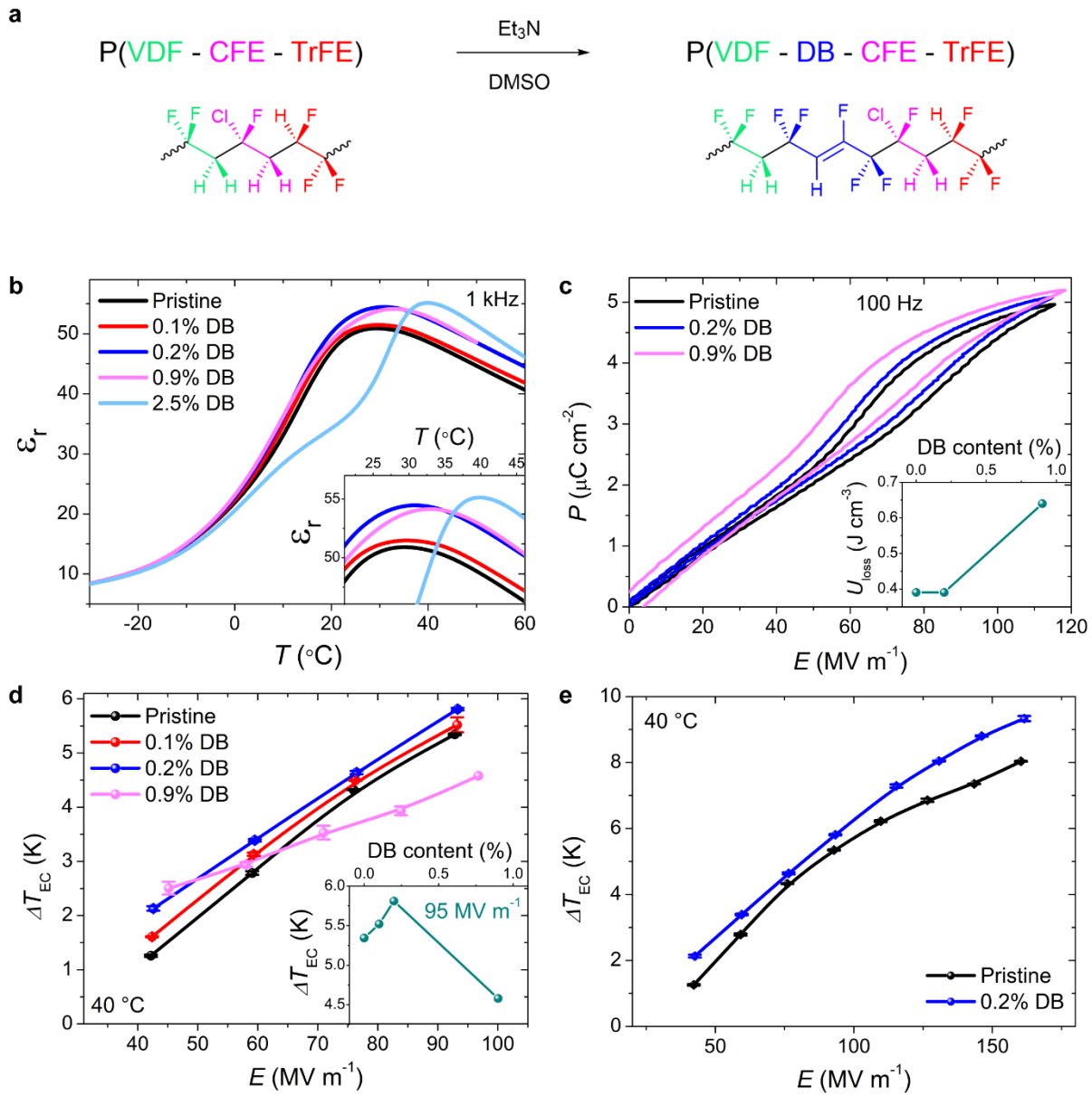

Figure 1. a) Structure of the pristine and DB-modified P(VDF-*ter*-TrFE-*ter*-CFE) terpolymers. Comparison of the dielectric and electrocaloric properties measured on the pristine and modified P(VDF-*ter*-TrFE-*ter*-CFE) terpolymers with various contents of double bonds: **b**) Real part of the permittivity *vs*. temperature at 1 kHz, **c**) polarization *vs*. electric field (*P-E* loops) measured at 100 Hz and 40 °C, with a maximum field of 120 MV·m^{-1}, **d**) direct electrocaloric adiabatic temperature change ΔT_{EC} *vs*. electric field *E* at 40 °C and E < 100 MV·m^{-1}, and **e**) ΔT_{EC} *vs*. *E* at 40 °C and high *E*. The inset of **c**) shows the evolution of the

hysteretic losses *vs*. double bonds content. The inset of **d**) shows the evolution of the maximum adiabatic temperature change *vs*. double bonds content, measured for E ~ 95 MV·m^{-1}.

An enhancement of the electrocaloric effect is induced in the DB-modified P(VDF-*ter*-TrFE-*ter*-CFE), as expected from the increased dielectric performance. A direct measurement of the adiabatic electrocaloric temperature change, ΔT_{EC}, near room temperature at a moderate electric field of 60 MV·m^{-1}, reveals an augmentation from ΔT_{EC} = 2.8 K for the pristine terpolymer to ΔT_{EC} = 3.1 K, ΔT_{EC} = 3.4 K and ΔT_{EC} = 3 K, for the for 0.1% DB, 0.2% DB and 0.9% DB-modified polymers, respectively (40 °C, Fig. 1d). The highest electrocaloric response at moderate electric fields (E < 100 MV·m^{-1}), ΔT_{EC} = 5.8 K is measured on the 0.2% DB-modified polymer at 95 MV·m^{-1}. This ranks among the best EC performance reported to date by direct measurements at moderate electric fields, with most reported values being ~ 5 K (see Table S2, Supporting Information). A notable exception was reported by Chen et al. with ΔT_{EC} = 8 K measured at 100 MV·m^{-1} in a fluorinated tetrapolymer.[23] However, the production of such niche polymer requires a significant and expensive synthetic effort, whereas our approach is based on the modification of a commercially-available polymer. A further increase of the DB content proves detrimental to the ECE in this electric field range with ΔT_{EC} decreasing to 4.5 K in the 0.9% DB-modified polymer. This trend is most probably the result of the increased hysteresis measured for this composition above 60 MV·m^{-1}, which significantly limits the field-induced entropy change, and thus the ECE, when the polymer-based capacitor is discharged. As ΔT_{EC} is proportional to the electric-field induced polarization change $P_{max}^2 - P_r^2$,[20] the slightest increase in P_r can drastically limit the electrocaloric response. An investigation at higher fields on the compositions with low hysteresis, reveals a remarkably high electrocaloric response in the 0.2% DB-modified polymer, with ΔT_{EC} = 9.3 K measured at 160 MV·m^{-1}.

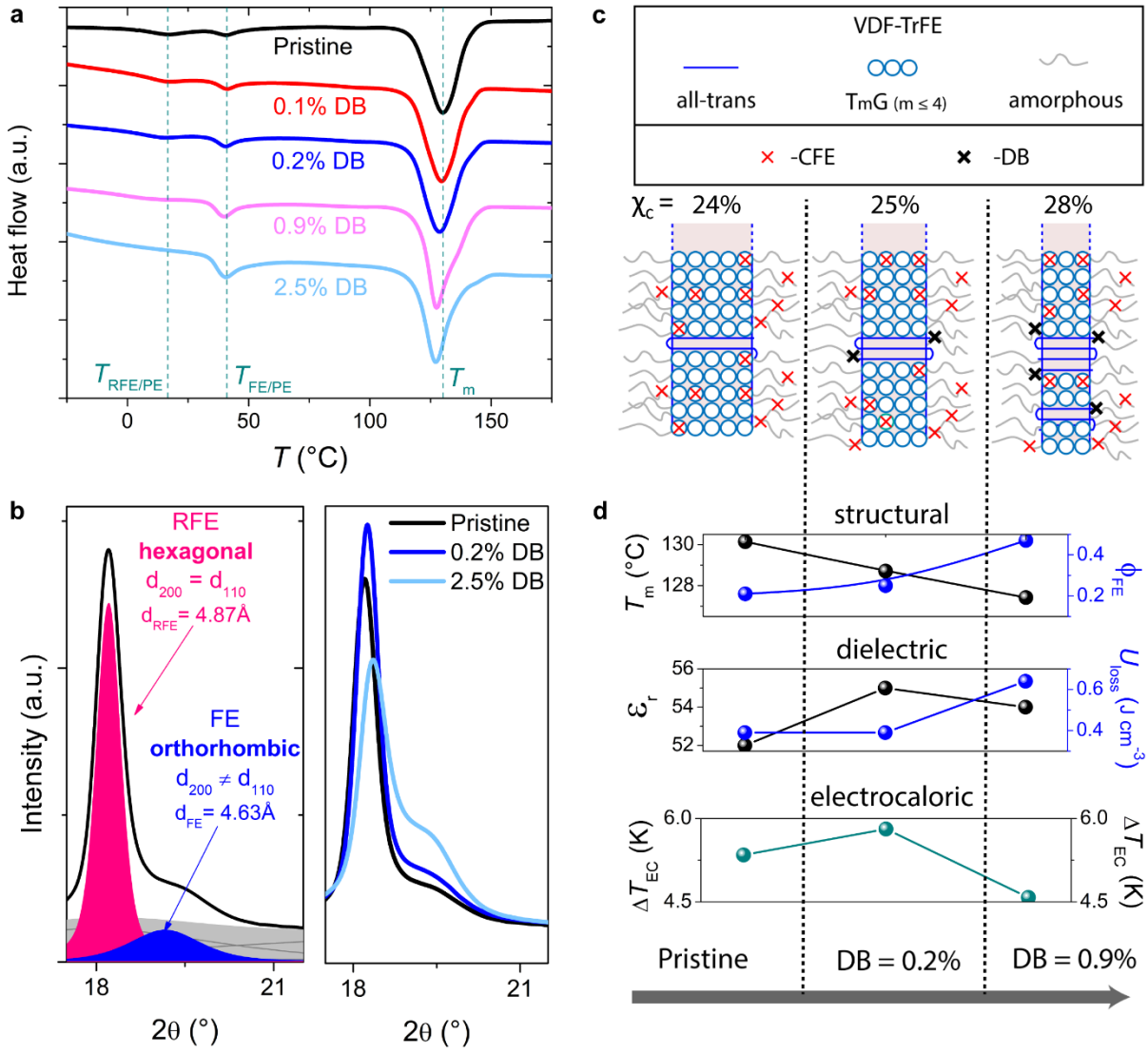

Figure 2. Evolution of the structural parameters of the pristine and modified P(VDF-*ter*-TrFE-*ter*-CFE) terpolymers with various contents of double bonds: **a**) Differential scanning calorimetry thermograms (first heating, 10 °C·min^{-1}). The dotted lines mark the temperature of the transitions in the pristine terpolymer. **b)** WAXS spectra measured on a pristine P(VDF-*ter*-TrFE-*ter*-CFE) polymer, where the crystalline (pink and blue) and amorphous (grey) contributions are decomposed as indicated (left panel). WAXS spectra measured at RT on the pristine P(VDF-*ter*-TrFE-*ter*-CFE) and its modified counterparts of different DB contents (right panel). **c**) Schematic representation of the evolution of the crystalline lamellae with increasing DB content (not to scale), with the corresponding weight average crystallinity (χ_c). **d**) Effect of the changes in the main structural parameters (melting temperature, T_m, and ferroelectric phase content, φ_{FE}) on the dielectric (permittivity, ε_r, and hysteretic losses, U_{loss}) and the resulting electrocaloric properties (ΔT_{EC}).

The structural origin of the enhanced dielectric and electrocaloric properties was elucidated by combining a suite of structural characterisation techniques. Information on the crystalline phases of these semi-crystalline polymers was obtained by differential scanning calorimetry (DSC, Fig. 2a) and Wide-angle X-Ray scattering (WAXS, Fig. S2). DSC revealed a depression of the melting temperature, T_m, with increasing DB-content (Fig. 2a, Table 1). As T_m is directly correlated to the lamellar thickness via the Gibbs-Thomson equation,[24,25] this trend is indicative of a thinning of the crystalline lamellae induced by the DB insertion, similarly to what we observed on modified P(VDF-*ter*-TrFE-*ter*-CTFE).[4] It most probably results from the decreased chain mobility around the DB, which hinders lamellar thickening. The crystallinity, proportional to the enthalpy of the melting peak ΔH_m was not significantly affected by the DB insertion, although a slight increase was observed. This trend was also confirmed by the WAXS data (weight average crystallinity, χ_c, Table 1). WAXS also provides information on the nature and amount of crystalline phases in the polymer. Two crystalline phases were identified in the series of studied compositions: a dense all-*trans*-rich ferroelectric phase with orthorhombic symmetry, referred to as FE, and a relaxor ferroelectric phase with hexagonal symmetry, referred to as RFE, with a predominantly gauche containing T_mG ($m \leq 4$) chain conformation, as expected from previous studies on similar polymers (Fig. 2b).[4,20,26] The orthorhombic FE phase is much denser (d_{FE} = 4.63 Å) than the hexagonal RFE phase, which shows an interplanar distance, d_{RFE} = 4.87 Å, close to that of the reported value for the high-temperature hexagonal paralectric (PE) phase (d_{PE} > 4.90 Å). In addition to the melting peak, two lower temperature features can be observed on the DSC thermograms. They correspond to the transition to the paraelectric behaviour of the RFE phase, T_{RFE}, and the FE phase, T_{FE}, near 20 °C and 45 °C, respectively, for the pristine terpolymer. The enthalpy of these transitions, ΔH_{RFE} and ΔH_{FE}, are indicative of the amount of each crystalline phase present in the polymer. The all-*trans*-rich FE

phase content was found to increase with increasing DB concentration, with the ratio ΔH_{FE} / ΔH_t, going from 0.39 to 0.88, for the pristine and 0.9%-DB-modified terpolymers, respectively ($\Delta H_t = \Delta H_{FE} + \Delta H_{RFE}$). This trend was confirmed by the WAXS data (FE content, φ_{FE}, increasing with DB amount, Table 1). The continuous growth of the FE phase with increasing DB content, at the expense of the RFE phase, which is quite clear in Fig. 2b (right panel), is indicative of phase competition rather than a simple two-phase mixture. Only three compositions are shown in Fig. 2b for the sake of clarity, but all the WAXS data and detailed peak attributions are provided in Fig. S2. A good agreement was obtained from FTIR measurements performed in the same conditions, which clearly displays an increase of the vibrations associated to all-*trans* chain conformation (1275 cm^{-1}, Fig. S3) to the detriment of the T_mG ($m \leq 4$) chain conformation (614 cm^{-1}, associated to the α-phase of PVDF[27]). The interplanar distance of the RFE phase, d_{RFE}, was found to gradually decrease with the DB content, which is also consistent with the densification arising from the stabilisation of some polymer chains with all-*trans* conformations inside the RFE crystalline lamellae. The interplanar distance of the FE phase, d_{FE}, remained unchanged.

Table 1: Structural parameters extracted from the differential scanning calorimetry (DSC) and Wide-angle X-Ray scattering (WAXS).

DB	**DSC**							**WAXS**			
[%]	T_m [°C]	ΔH_m [J g^{-1}]	T_{FE} [°C]	ΔH_{FE} [J g^{-1}]	T_{RFE} [°C]	ΔH_{RFE} [J g^{-1}]	ΔH_{FE} / ΔH_t	χ_c [%]	φ_{FE} [%]	d_{FE} [Å]	d_{RFE} [Å]
0	130.1	22.7	41	0.7	16.6	1.1	0.39	24	21	4.63	4.87
0.1	129.4	24.1	40.9	1.1	15.6	1.4	0.44	25	21	4.63	4.87
0.2	128.7	23.7	40.6	1.4	13.9	1.1	0.56	25	25	4.63	4.86
0.9	127.4	23.1	40	2.4	6.6	0.9	0.74	28	47	4.63	4.84
2.5	127	20.3	40.5	4.6	1.3	0.6	0.88	27	47	4.63	4.83

Thus, the insertion of DB on the terpolymers' backbone induces two main structural modifications, which are schematically summarized in Fig. 2c:

- The lamellar thickening is hindered during the crystallisation of the crystalline lamellae, most probably due to an accumulation of the double bonds at the crystalline/amorphous interfaces, where the -CFE groups are predominant in the pristine polymer.
- A gradual stabilisation of the all-*trans* containing crystalline phase, which results from the decrease of the gauche-stabilizing -CFE content, induced by the dehydrochlorination during the DB formation.

The evolution of these structural parameters can be directly correlated to the electrocaloric enhancement in the DB-modified P(VDF-*ter*-TrFE-*ter*-CFE). The decrease of the lamellar thickness, confirmed by the decrease of T_m, leads to an enhancement of the permittivity, ε_r, and thus of the maximum polarisation, P_{max}. Concomitantly, low hysterestic losses, U_{loss}, and thus low remanent polarisation, P_r, are maintained in the 0.2% DB-modified polymers, because the increase of the all-*trans* containing crystalline phase, φ_{FE}, remains limited. Both of these trends (summarised schematically in Fig. 2c) contribute to the increase of ΔT_{EC} , which is proportional to the electric-field induced polarization change $P_{max}^2 - P_r^2$.[20]

Broadband dielectric spectroscopy (BDS) was used to further quantify the effect of DB introduction on the structure of P(VDF-*ter*-TrFE-*ter*-CFE) and elucidate the origin of the dielectric enhancement. Similarly to other relaxor ferroelectrics such as inorganic oxide perovkites, including PMN-PT,[28] a broad and dispersive permittivity peak is observed in pristine P(VDF-*ter*-TrFE-*ter*-CFE) (63/30/7), as shown in Fig. 3a, which is in good agreement with the low enthalpy values measured by DSC for this diffuse phase transition (ΔH_{RFE}, Table 1). This behaviour results from the presence of polar nano-regions (PNRs) in relaxor ferroelectrics, which are less correlated than polar domains in conventional ferroelectrics,

where a long-range order can be established resulting in a high remanent polarisation. While PNRs can be strongly polarized and thus induce high macroscopic polarization, this correlation is lost upon removing the electric field,[1,11,28] as highlighted by the low remanent polarisation displayed in Fig. 1c. Still, the interactions between these PNRs increase with decreasing temperature and a static "freezing" temperature, T_f, is eventually reached where these interactions become high enough to induce a remanant polarization. Near this temperature, the dielectric relaxation time abruptly increases thus inducing a "super-Arrhenius" behaviour, with similarities to the super-cooled liquid observed below the glass transition of polymer.[29,30] Due to these similarities, it has been accepted that the dielectric relaxation in relaxor ferroelectric can be described with a Vogel-Fulcher (VF) equation :[16,28]

$$f = f_0 \exp\left(\frac{-E_a}{k_B\,(T_{max} - T_f)}\right) \quad (1)$$

Where f_0 the high-temperature limit frequency, E_a the activation energy, k_B the Boltzmann constant, and T_{max} the temperature of maximum permittivity for each frequency f.

The Ln f with $1/T_{max}$ curves, extracted from the BDS data for the pristine terpolymer (Fig. 3a) and the DB-modified polymers (Fig. S4), are presented in Fig. 3b. A clear "super-Arrhenius" behaviour was observed for all compositions with a good agreement between the measured data and the VF fit. The activation energy extracted from the VF fit is displayed as a function of DB content in Fig. 3c. It clearly shows a gradual decrease of E_a with increasing DB content. This E_a is the activation energy for polarization fluctuation of an isolated PNR, which needs to be overcome in order to develop short-range order between the PNRs and thus induce a large macroscopic polarisation upon electric field application. The abrupt decrease of E_a with increasing DB content, combined with the competition between the two crystallographic phases (orthorhombic FE and hexagonal RFE) evidenced by the structural characterisations data, suggests that the introduction of DB induces a morphotropic phase boundary (MPB) in the

polymer, similar to the one reported by Liu et al. in P(VDF-*co*-TrFE) (50/50).[16] The MPB in P(VDF-*co*-TrFE) marks a crossover region of competition between an orthorhombic FE phase (VDF-rich side) and a pseudo-hexagonal RFE phase (TrFE-rich side), with lattice parameters (interplanar distances) close to that of the hexagonal paraelectric phase. In P(VDF-*ter*-TrFE-*ter*-CFE), the MPB involves similar crystallographic phases, but it is much more RFE-rich than in P(VDF-*co*-TrFE), due the large CFE groups, which favour the formation the gauche defects with T_mG ($m \leq 4$) chain conformation, and thus the crystallisation of phases with higher interplanar distances, even for the orthorhombic FE phase. The presence of this MPB coincides well with the decrease of the melting temperature, T_m, and the increase of the FE crystalline phase content in the otherwise RFE-dominant terpolymer (see Fig. 3d and Fig. 2b). Therefore, the decrease in activation energy is most probably the result of the nucleation of all-*trans* polymer chains inside the T_mG ($m \leq 4$) regions, which facilitates the field-induced rotation from T_mG ($m \leq 4$) to all-*trans* required to induce a large dipole moment in each polar cluster. The coexistence of these phases decreases the energy barrier to rotate from T_mG ($m \leq 4$) to all-*trans*, and thus the energy required to polarise the material, leading to a region of enhanced dielectric properties. In that regard, the newly formed all-*trans*-rich RFE phase plays a similar role to the intermediate monoclinic phase in the MPB of inorganic perovskites, such as PMN-PT, which facilitates dipole rotation from the orthorhombic to the tetragonal phase.[6] This dipole alignment in DB-P(VDF-*ter*-TrFE-*ter*-CFE) is further facilitated by the thinning of the crystalline lamellae, which decreases the inter-lamellar interactions and facilitates intra-lamellar polymer chain rotations.

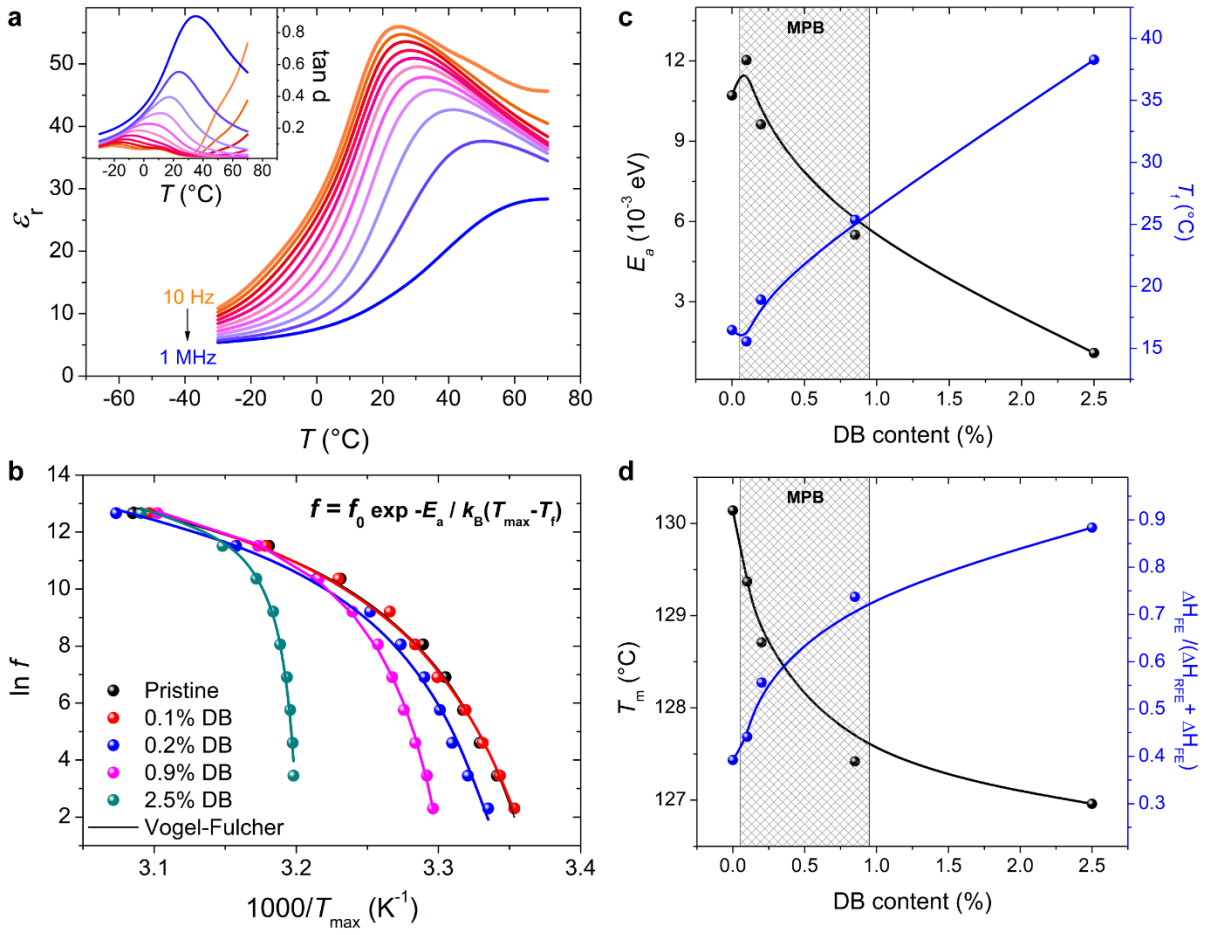

Figure 3. Broadband dielectric spectroscopy versus temperature measured on P(VDF-*ter*-TrFE-*ter*-CFE): **a**) real part of the permittivity and loss tangent (inset). **b**) Relaxation frequency *vs*. inverse temperature and Vogel-Fulcher (VF) fit for the pristine and modified terpolymer with various contents of double bonds. **c**) VF-extracted activation energy and freezing temperature *vs*. double bond content. **d**) Melting temperature and phase transition enthalpy ratio *vs*. double bond content, obtained from DSC.

The MPB extends to 0.9% DB, where a permittivity enhancement was also measured, and possibly beyond, however, the increase of the correlation between the polar clusters also results in an increase of the freezing temperature T_f (17-20 °C for the pristine, 0.1 % DB, and 0.2 % DB modified polymers, 25°C for 0.9 % of DB and 38°C for 2.5% of DB). This higher T_f , which results from the growth of the dense all-*trans*-rich orthorhombic FE phase, strengthens the polar correlation between the PNRs near room temperature. It leads to higher remanent polarisation

and thus larger hysteresis, which has a detrimental effect on the ECE, as demonstrated in Fig. 1d for the 0.9 % DB modified polymers. Therefore, as P(VDF-*ter*-TrFE-*ter*-CFE) is already well optimised for room temperature application, the compositional range where the dielectric and electrocaloric properties can be further enhanced is quite narrow and only minute amounts of unsaturation should be used.

The potential of these modified polymers for the cooling of flexible features in wearable electronics was investigated by measuring the polarisation of the polymer-based flexible capacitors bent with different curvature angles. Fig. 4a shows the results of this study on the 0.9 % DB modified polymer. Several angles were tested by bending flexible capacitors (with a 38-mm^2 surface area) on cylinders of different diameters, in order to emulate different curvatures (the method to estimate the curvature angle is given in Fig. S5). A curvature angle, $\alpha = 4°$, is realistic for a wrist-size sensor (Fig. 4b), while $\alpha = 14°$, is more adapted to a sensor wrapped around a finger (Fig. 4c). In all cases, the performance (polarisation versus electric field) of the polymer remains unaffected, and in good agreement with the data presented in Fig. 1c for E up to 50 $MV \cdot m^{-1}$, regardless of the angle of curvature. While the modified DSC method tool used for direct ECE measurements is unsuitable to characterise the performances of bent samples, the aforementioned direct correlation between polarisation and electrocaloric response suggests that the ECE is unaffected by the changes in curvature angles studied here, thus highlighting the great promise of these flexible polymer-based capacitors in wearable electronics.

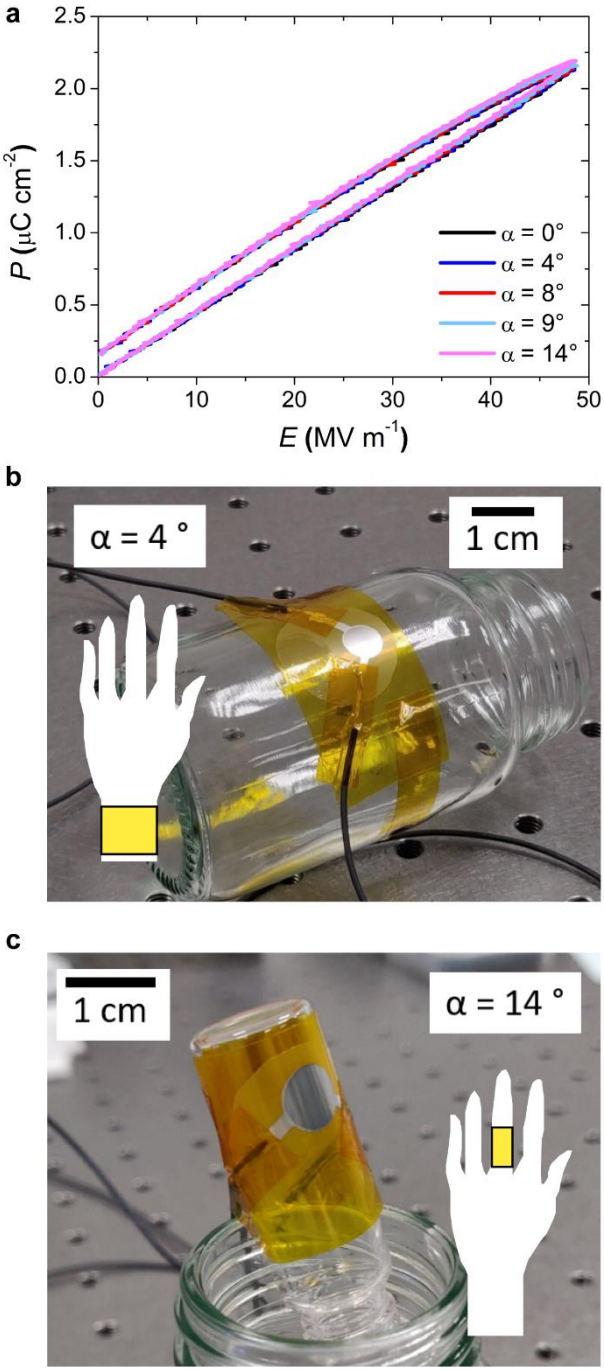

Figure 4. Effect of curvature angle of bending on the high-field dielectric properties of 0.9%DB-modified P(VDF-*ter*-TrFE-*ter*-CFE): **a**) Polarisation versus electric field measured at 25 °C with a maximum field E = 50 MV·m^{-1} for flexible samples bent with various curvature angles. Photograph and schematic representation of flexible devices bent with curvature angles corresponding to **b**) a wrist (α = 4°) and **c**) a finger (α = 14°).

Conclusions

In summary, we have induced a morphotropic phase boundary (MPB) in flexible P(VDF-*ter*-TrFE-*ter*-CFE) devices, leading to increased dielectric properties near room temperature, and enhanced electrocaloric effect. This was achieved with a one-pot chemical modification of the terpolymers, in which minute amounts of unsaturation were introduced on the backbone of the semi-crystalline terpolymers. The DBs induced a depression of the melting temperature, associated with a thinning of the crystalline lamellae, and stabilized a fraction of more polar all-*trans* polymer chain configuration, in the vicinity of which dipole rotation is facilitated upon electric field application. This resulted in a decrease of the activation energy to flip between equivalent dipolar directions typically observed near a MPB. The modified polymers achieved remarkable electrocaloric performance at 40 °C, with ΔT_{EC} = 5.8 K at low fields E < 100 MV·m^{-1}, and up to 9.3 K measured at higher fields in the 0.2%-DB P(VDF-*ter*-TrFE-*ter*-CFE) polymer. The MPB extended to more DB-rich compositions, with enhanced permittivity measured in the 0.9%-DB P(VDF-*ter*-TrFE-*ter*-CFE) polymer as well. However, the concomitant increase in freezing temperature observed for higher DB contents, resulting in higher polar correlation, and thus stronger polarization hysteresis, proved detrimental to the cooling properties. Finally, we showed that the enhanced dielectric properties observed in these flexible devices remained unaffected when subjected to conditions of bending and curvature typical of sensors worn on the human body, thus highlighting the great promise of these flexible polymer-based capacitors in wearable electronics.

Supporting Information

Supporting Information is available free of charge via the Internet at http://pubs.acs.org. All experimental details are included, with the description of the materials used, the methods for

film and device fabrication, as well as detailed procedures and lists of the instruments and characterization techniques used to obtain the results presented here. Also included are the structure of the neat and DB-modified P(VDF-*ter*-TrFE-*ter*-CFE) terpolymers and the reaction mechanism of the dehydrochlorination (Scheme S1), the H^1-NMR spectra (Fig. S1), the reaction conditions used for the chemical modifications of each polymer studied here (Table S1). A table listing the best reported adiabatic temperature changes measured on polymer-based devices for $E \leq 100$ MV·m^{-1} is provided (Table S2), as well the WAXS spectra and their deconvolution (Fig. S2) and the FTIR spectra (Fig. S3). Finally, are included the broadband dielectric spectroscopy study for all polymers (Fig. S4), as well as a detailed description of the curvature angle α used to study the influence of bending on the dielectric properties (Fig. S5).

Acknowledgements

K.K. acknowledges the Région Nouvelle Aquitaine for the financial support (Ph.D. grant #2015-1R10207-00004862). This work was performed within the framework of the of the ANR Industrial Chair "SMILE" (ANR-19-CHIN-0002) and the Equipex ELORPrintTec ANR-10-EQPX-28-01 with the help of the French state's Initiative d'Excellence IdEx ANR-10-IDEX-003-02. S.T.-G's contribution was achieved within the framework of the Industrial Chair Arkema (Arkema/CNRS-ENSAM-Cnam).

Conflict of interest

The authors declare no conflict of interest.

References

(1) Correia, T.; Zhang, Q. *Electrocaloric Materials*; Engineering Materials; Springer: Berlin, Heidelberg, 2014, 184-191.

(2) Monch, S.; Reiner, R.; Mansour, K.; Waltereit, P.; Basler, M.; Quay, R.; Molin, C.; Gebhardt, S.; Bach, D.; Binninger, R.; et al. A 99.74% Efficient Capacitor-Charging Converter Using Partial Power Processing for Electrocalorics. *IEEE J. Emerg. Sel. Top. Power Electron.* **2023**, *11* (4), 4491 – 4507. https://doi.org/10.1109/JESTPE.2023.3270375.

(3) Shi, J.; Han, D.; Li, Z.; Yang, L.; Lu, S.-G.; Zhong, Z.; Chen, J.; Zhang, Q. M.; Qian, X. Electrocaloric Cooling Materials and Devices for Zero-Global-Warming-Potential, High-Efficiency Refrigeration. *Joule* **2019**, *3* (5), 1200–1225. https://doi.org/10.1016/J.JOULE.2019.03.021.

(4) Le Goupil, F.; Kallitsis, K.; Tencé-Girault, S.; Pouriamanesh, N.; Brochon, C.; Cloutet, E.; Soulestin, T.; Domingue Dos Santos, F.; Stingelin, N.; Hadziioannou, G. Enhanced Electrocaloric Response of Vinylidene Fluoride–Based Polymers via One-Step Molecular Engineering. *Adv. Funct. Mater.* **2021**, *31* (1), 2007043. https://doi.org/10.1002/adfm.202007043.

(5) Kutnjak, Z.; Petzelt, J.; Blinc, R. The Giant Electromechanical Response in Ferroelectric Relaxors as a Critical Phenomenon. *Nature* **2006**, *441* (7096), 956–959. https://doi.org/10.1038/nature04854

(6) Noheda, B.; Cox, D. E.; Shirane, G.; Gao, J.; Ye, Z.-G. G. Phase Diagram of the Ferroelectric Relaxor (1-x)PbMg1/3Nb2/3O3-xPbTiO3. *Phys. Rev. B* **2002**, *66* (5), 1–10. https://doi.org/05410410.1103/PhysRevB.66.054104.

(7) Keeble, D. S.; Benabdallah, F.; Thomas, P. A.; Maglione, M.; Kreisel, J. Revised Structural Phase Diagram of (Ba0.7Ca0.3TiO3)-(BaZr0.2Ti0.8O3). *Appl. Phys. Lett.* **2013**, *102* (9), 92903. https://doi.org/10.1063/1.4793400.

(8) Walker, J.; Simons, H.; Alikin, D. O.; Turygin, A. P.; Shur, V. Y.; Kholkin, A. L.; Ursic, H.; Bencan, A.; Malic, B.; Nagarajan, V.; et al. Dual Strain Mechanisms in a Lead-Free Morphotropic Phase Boundary Ferroelectric. *Sci. Reports* **2016**, *6* (1), 1–8. https://doi.org/10.1038/srep19630.

(9) Otoničar, M.; Bradeško, A.; Fulanović, L.; Kos, T.; Uršič, H.; Benčan, A.; Cabral, M. J.; Henriques, A.; Jones, J. L.; Riemer, L.; et al. Connecting the Multiscale Structure with Macroscopic Response of Relaxor Ferroelectrics. *Adv. Funct. Mater.* **2020**, *30* (52), 2006823. https://doi.org/10.1002/ADFM.202006823.

(10) Le Goupil, F.; Berenov, A.; Axelsson, A.-K.; Valant, M.; Alford, N. M. Direct and Indirect Electrocaloric Measurements on 〈001〉-PbMg1/3Nb2/3O3-30PbTiO3 Single Crystals. *J. Appl. Phys.* **2012**, *111* (12), 124109. https://doi.org/10.1063/1.4730338

(11) Le Goupil, F.; Axelsson, A.-K.; Dunne, L. J.; Valant, M.; Manos, G.; Lukasiewicz, T.; Dec, J.; Berenov, A.; Alford, N. M. Anisotropy of the Electrocaloric Effect in Lead-Free Relaxor Ferroelectrics. *Adv. Energy Mater.* **2014**, *4* (9), 1301688. https://doi.org/10.1002/aenm.201301688.

(12) Qian, X.-S.; Ye, H.-J.; Zhang, Y.-T.; Gu, H.; Li, X.; Randall, C. A.; Zhang, Q. M. Giant Electrocaloric Response over a Broad Temperature Range in Modified BaTiO3 Ceramics. *Adv. Funct. Mater.* **2014**, *24* (9), 1300–1305. https://doi.org/10.1002/adfm.201302386.

(13) Otoničar, M.; Dkhil, B. Electrocalorics Hit the Top. *Nat. Mater.* **2019**, *19* (1), 9–11. https://doi.org/10.1038/s41563-019-0522-1.

(14) Geng, W.; Liu, Y.; Meng, X.; Bellaiche, L.; Scott, J. F.; Dkhil, B.; Jiang, A. Giant Negative Electrocaloric Effect in Antiferroelectric La-Doped Pb(ZrTi)O3 Thin Films Near Room Temperature. *Adv. Mater.* **2015**, *27* (20), 3165–3169. https://doi.org/10.1002/ADMA.201501100.

(15) Rozic, B.; Kosec, M.; Ursic, H.; Holc, J.; Malic, B.; Zhang, Q. M.; Blinc, R.; Pirc, R. R.; Kutnjak, Z. Influence of the Critical Point on the Electrocaloric Response of Relaxor Ferroelectrics. *J. Appl. Phys.* **2011**, *110* (6), 64115–64118. https://doi.org/10.1063/1.3641975.

(16) Liu, Y.; Han, Z.; Xu, W.; Haibibu, A.; Wang, Q. Composition-Dependent Dielectric Properties of Poly(vinylidene Fluoride-Trifluoroethylene)s near the Morphotropic Phase Boundary. *Macromolecules* **2019**, *52* (17), 6741–6747. https://doi.org/10.1021/ACS.MACROMOL.9B01403.

(17) Liu, Y.; Aziguli, H.; Zhang, B.; Xu, W.; Lu, W.; Bernholc, J.; Wang, Q. Ferroelectric Polymers Exhibiting Behaviour Reminiscent of a Morphotropic Phase Boundary. *Nature* **2018**, *562* (7725), 96–100. https://doi.org/10.1038/s41586-018-0550-z.

(18) Ma, R.; Zhang, Z.; Tong, K.; Huber, D.; Kornbluh, R.; Ju, Y. S.; Pei, Q. Highly Efficient Electrocaloric Cooling with Electrostatic Actuation. *Science* **2017**, *357* (6356), 1130–1134. https://doi.org/10.1126/science.aan5980.

(19) Arman Kuzubasoglu, B.; Kursun Bahadir, S. Flexible Temperature Sensors: A Review. *Sensors Actuators, A Phys.* **2020**, *315*, 112282. https://doi.org/10.1016/J.SNA.2020.112282.

(20) Le Goupil, F.; Coin, F.; Pouriamanesh, N.; Fleury, G.; Hadziioannou, G. Electrocaloric Enhancement Induced by Cocrystallization of Vinylidene Difluoride-Based Polymer Blends. *ACS Macro Lett.* **2021**, *10* (12), 1555–1562. https://doi.org/10.1021/acsmacrolett.1c00576.

(21) Fricaudet, M.; Žiberna, K.; Salmanov, S.; Kreisel, J.; He, D.; Dkhil, B.; Rojac, T.; Otoničar, M.; Janolin, P.-E.; Bradeško, A. Multifunctional Properties of Polyvinylidene-Fluoride-Based Materials: From Energy Harvesting to Energy Storage. *ACS Appl. Electron. Mater.* **2022**, *4* (11), 5429–5436. https://doi.org/10.1021/acsaelm.2c01091.

(22) Qian, X.; Han, D.; Zheng, L.; Chen, J.; Tyagi, M.; Li, Q.; Du, F.; Zheng, S.; Huang, X.; Zhang, S.; et al. High-Entropy Polymer Produces a Giant Electrocaloric Effect at Low Fields. *Nature* **2021**, *600* (7890), 664–669. https://doi.org/10.1038/s41586-021-04189-5.

(23) Chen, X.; Xu, W.; Lu, B.; Zhang, T.; Wang, Q.; Zhang, Q. M. Towards Electrocaloric Heat pump—A Relaxor Ferroelectric Polymer Exhibiting Large Electrocaloric Response at Low Electric Field. *Appl. Phys. Lett.* **2018**, *113* (11), 113902. https://doi.org/10.1063/1.5048599.

(24) Gibbs, J. W.; Bumstead, H. A.; Van Name, R. G.; Longley, W. R. *The Collected Works of J. Willard Gibbs*; Longmans, Green and Co., 1902.

(25) Thomson, J. J. *Applications of Dynamics to Physics and Chemistry*; Adamant Media Corporation, 2005.

(26) Bargain, F.; Thuau, D.; Panine, P.; Hadziioannou, G.; Domingues Dos Santos, F.; Tencé-Girault, S. Thermal Behavior of poly(VDF-Ter-TrFE-Ter-CTFE) Copolymers: Influence of CTFE Termonomer on the Crystal-Crystal Transitions. *Polymer* **2019**, *161*, 64–77. https://doi.org/10.1016/J.POLYMER.2018.11.064.

(27) Cai, X.; Lei, T.; Sun, D.; Lin, L. A Critical Analysis of the A, β and γ Phases in Poly(vinylidene Fluoride) Using FTIR. *RSC Adv.* **2017**, *7* (25), 15382–15389. https://doi.org/10.1039/C7RA01267E.

(28) Viehland, D.; Jang, S. J.; Cross, L. E.; Wuttig, M. Freezing of the Polarization Fluctuations in Lead Magnesium Niobate Relaxors. *J. Appl. Phys.* **1998**, *68* (6), 2916. https://doi.org/10.1063/1.346425.

(29) Levit, R.; Martinez-Garcia, J. C.; Ochoa, D. A.; García, J. E. The Generalized Vogel-Fulcher-Tamman Equation for Describing the Dynamics of Relaxor Ferroelectrics. *Sci. Reports* **2019**, *9* (1), 1–8. https://doi.org/10.1038/s41598-019-48864-0.

(30) Böhmer, R.; Ngai, K. L.; Angell, C. A.; Plazek, D. J. Nonexponential Relaxations in Strong and Fragile Glass Formers. *J. Chem. Phys.* **1993**, *99* (5), 4201. https://doi.org/10.1063/1.466117.

Table of Contents

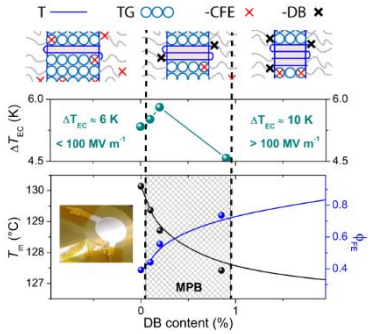

for Table of Contents use only